Multilevel voltage source inverter with coupled reactors using coarsely quantized pulse amplitude modulation

Krzysztof Jakub SZWARC[1] [iD]*, Artur CICHOWSKI[1] [iD], Paweł SZCZEPANKOWSKI[1] [iD],

Janusz NIEZNAŃSKI[1] [iD], and Ryszard STRZELECKI[1, 2] [iD]

[1] Gdańsk University of Technology, Gdańsk, Poland
[2] Gdynia Maritime University, Gdynia, Poland

Abstract. The paper discusses a multilevel voltage source inverter with coupled reactors (MVSI-CR). The output voltage is generated using the novel coarsely quantized pulse amplitude modulation (CQ-PAM). The AC voltage synthesis is realized by selecting and applying an appropriate collection of voltage vectors from the space-vector diagram. Integrating classical two-level inverters allows for achieving modularity of the solution. The main advantage of the proposed approach is a very low switching-to-fundamental frequency ratio and a multistep quasi-sinusoidal output voltage. The paper includes a theoretical analysis, simulations, and laboratory test results.

Keywords: multi-level inverter; pulse amplitude modulation; coupled reactors; multi-pulse; voltage source inverter.

1. INTRODUCTION

Most of the modern DC-AC converters need pulse width modulation (PWM) techniques and passive filters to obtain sinusoidal output voltages. As a result, high switching frequencies – several kilohertz or more – are usually required, leading to high switching losses and considerable electromagnetic interference (EMI). Despite the latest developments in power electronic devices, the problem of high-frequency operation remains a challenge. The use of conventional PWM techniques tends to be particularly problematic in high-speed drive applications where the speed can reach 500 000–1 000 000 rpm at 1 kW [1, 2] or 100 000 rpm at 60 kW [3] or 12 000–15 000 rpm for the powers above 1 MW [3]. The PWM can also be a source of problems in high-power ultrasound systems, welding applications, and food technology, and other applications.

Reducing the switching frequency of the power electronic devices without significant loss of the output voltage quality can be achieved by using multi-level voltage source inverters (MVSI), including the topologies based on the use of magnetic elements such as multi-phase transformers with an appropriately designed winding group [4]. A cost-effective solution can be the use of coupled reactors, whereby a significant size reduction can be achieved (compared to transformers) (for a given load power, the power to be handled by the coupled reactors will be around five times lower than in the case of a transformer [5]. The idea, first used in the multi-pulse diode rectifiers [6,7], was proposed

for inverter circuits in [8] (multilevel voltage source inverters with coupled reactors, MVSI-CR) where all VSI modules were integrated using a special magnetic circuit of coupled reactors.

In the basic operational mode of MVSI-CR presented in [9], the switches of the MVSI-CR commute at the frequency of the output voltage, which significantly reduces the switching losses and the EMI problems. In addition, the application of the conventional two-level inverter as an easily replaceable power module facilitates the maintenance of the converter. As was demonstrated in [9], this solution can be scaled up by adding another power module to the system and modifying the circuit of the coupled reactors. Moreover, a well-balanced power division can be obtained in the system as reported in [10], where a 12-pulse inverter topology was discussed. Another example of the multi-pulse topology can be found in [11] in the form of a 24-pulse STATCOM. It should be stressed that none of the systems referred to above offers the magnitude control of the output voltage.

A simple way to adjust the output voltage is the DC-link regulation. However, this solution needs additional DC-DC converter which complicates the construction and lowers the performance of the whole system. Therefore, this solution is only used in very specific applications [2]. Another method to control the output voltage is the PWM, but the attempts to use PWM for active rectifiers [12–14] did not bring the expected results. The main disadvantage of this solution is the relatively high switching frequency.

This paper discusses the output voltage control of the 18-pulse MVSI-CR using the proposed CQ-PAM method. This method allows rough adjustment of the output voltage while keeping the switching frequency relatively low. A brief introduction to multi-

K.J. Szwarc, A. Cichowski, P. Szczepankowski, J. Nieznański, and R. Strzelecki

pulse converters is presented in Section 2. Section 3 provides a closer look at the 18-pulse MVSI-CR. The CQ-PAM modulation is described in Section 4. The simulation results are discussed in Section 5, while the laboratory tests are presented in Section 6.

2. THE PRINCIPLE OF MULTI-PULSE CONVERTERS

Multi-pulse converters [15–17] provide higher efficiency and a lower distortion level of the generated waveforms than standard two-level converters [18–20]. These topologies have been applied in the passive diode rectifiers and the active transistor/thyristor rectifiers. Among them, the 12-pulse rectifiers [12, 13, 15] can be indicated as the most commonly used due to their simple construction. A greater number of pulses increases the overall complexity of the multi-pulse devices. However, the benefits are: decreasing distortion of the output voltages and increasing power quality. In general, the phase voltage of the p-pulse converter contains the following harmonics:

$$h = (n \cdot p) \pm 1, \tag{1}$$

where $n \in N$.

The 18-pulse and 24-pulse topologies were discussed in [16, 21, 22] and [23, 24], respectively, while rectifiers with a larger number of pulses were considered in [25, 26].

A common feature of the proposed topologies is the possibility of building the converter using conventional two-level modules. The p-pulse converter requires $k = \frac{p}{p_m}$ basic modules (for the three-phase system p_m is equal to 6) and other components, such as transformers [27–29], autotransformers [12, 21, 30] or coupled reactors [7, 31, 32]. The main advantages of the coupled reactors is the lower price and volume compared to the topologies using transformers or auto-transformers. A disadvantage is that the coupled reactors do not provide galvanic isolation.

The coupled reactor circuit parameters have to be adapted to the number of pulses. An important design parameter is the angle ϕ defined by

$$\phi = \frac{2 \cdot \pi}{p_m \cdot k} \tag{2}$$

and determining the shift between converter control signals. In particular, the required windings turns ratio for the coupled reactors can be calculated using this parameter. A variety of other parameters of the integrating elements depend on the specific requirements of the particular application (frequency, power, max voltage, symmetry or asymmetry). The discussion of these aspects is not covered in this paper.

3. THE MULTILEVEL VOLTAGE SOURCE INVERTER WITH COUPLED REACTORS

Multipulse topologies have also been proposed for the DC-AC conversion [9, 10]. The relatively low commutation frequency and the good quality of output signals are great advantages of these solutions. However, the complicated topology leads to difficulties in the control of the output voltage – and this is an aspect which has not received sufficient attention.

The total number of switching state combinations for the m-pulse inverter with an l-level module is $l^{\frac{m}{2}}$. The considered 18-pulse inverter consists of three two-level inverters, which means $2^9 = 512$ possible states. Using three-level inverter modules would result in $3^9 = 19\,683$ possible states.

Concerning the "m-pulse" qualifier used to define the converter topologies, it has a clear meaning in the case of diode or thyristor AC–DC converters (it indicates the number of sections of the input AC voltage, called "pulses", transferred to the DC output). For DC–AC inverters this idea of pulses is much less tangible, but can still be used as a constructional parameter of the inverter.

A complete schematic of the 18-pulse MVSI-CR is shown in Fig. 1, while Fig. 2 defines the vectorial notation of voltages used in the following analysis. The output voltage is generated using three two-level inverters and two kinds of coupled reactors: the phase shifters and the current mergers. The output voltage can be expressed as

$$\hat{V}_o = \hat{V}_{PS} + \Delta \hat{V}_3 . \tag{3}$$

The detailed analysis of the output voltage synthesis is presented in [33]. The phase shifters output voltages can be described by

$$\hat{V}_{PS} = \hat{V}_1 - \left(\hat{V}_1 - \hat{V}_2\right) \cdot \frac{N_A + N_B}{2 \cdot N_A + N_B}$$
$$- \left(\hat{V}_1 - \hat{V}_2\right) \cdot a^{-1} \cdot \frac{N_B}{2 \cdot N_A + N_B} , \tag{4}$$

where

$$\hat{V}_1 = U_M \cdot e^{j \frac{\pi}{3} \cdot ent \left[\frac{3}{\pi} (\omega t + \phi) \right]},$$
$$\hat{V}_2 = U_M \cdot e^{j \frac{\pi}{3} \cdot ent \left[\frac{3}{\pi} (\omega t - \phi) \right]}, \tag{5}$$
$$\hat{V}_3 = U_M \cdot e^{j \frac{\pi}{3} \cdot ent \left[\frac{3}{\pi} \omega t \right]}.$$

Considering the current mergers as voltage dividers, $\hat{V}_{PS}$ can be expressed by

$$\Delta \hat{V}_3 = \hat{V}_3 - \hat{V}_{PS} - \left(\hat{V}_3 - \hat{V}_{PS}\right) \cdot \frac{N_C}{N_C + N_D} . \tag{6}$$

Substituting the above relationship into equation (3), we obtain

$$\hat{V}_o = \hat{V}_3 - \left(\hat{V}_3 - \hat{V}_{PS}\right) \cdot \frac{N_C}{N_C + N_D} . \tag{7}$$

According to the analysis presented in [12, 33] for the 12-pulse topology, the required turns ratio of the reactor coils can be expressed by the following formulas:

$$\frac{N_A}{N_B} = \frac{\sin\left(\frac{2 \cdot \pi}{6} - \phi\right)}{\sin(\phi)}, \tag{8}$$
$$N_\Sigma = N_A + N_B ,$$

where N_Σ, N_A, and N_B represent the primary, secondary, and tertiary windings of the phase shifters, respectively. The turns ratios of the current mergers can be evaluated based on the

2

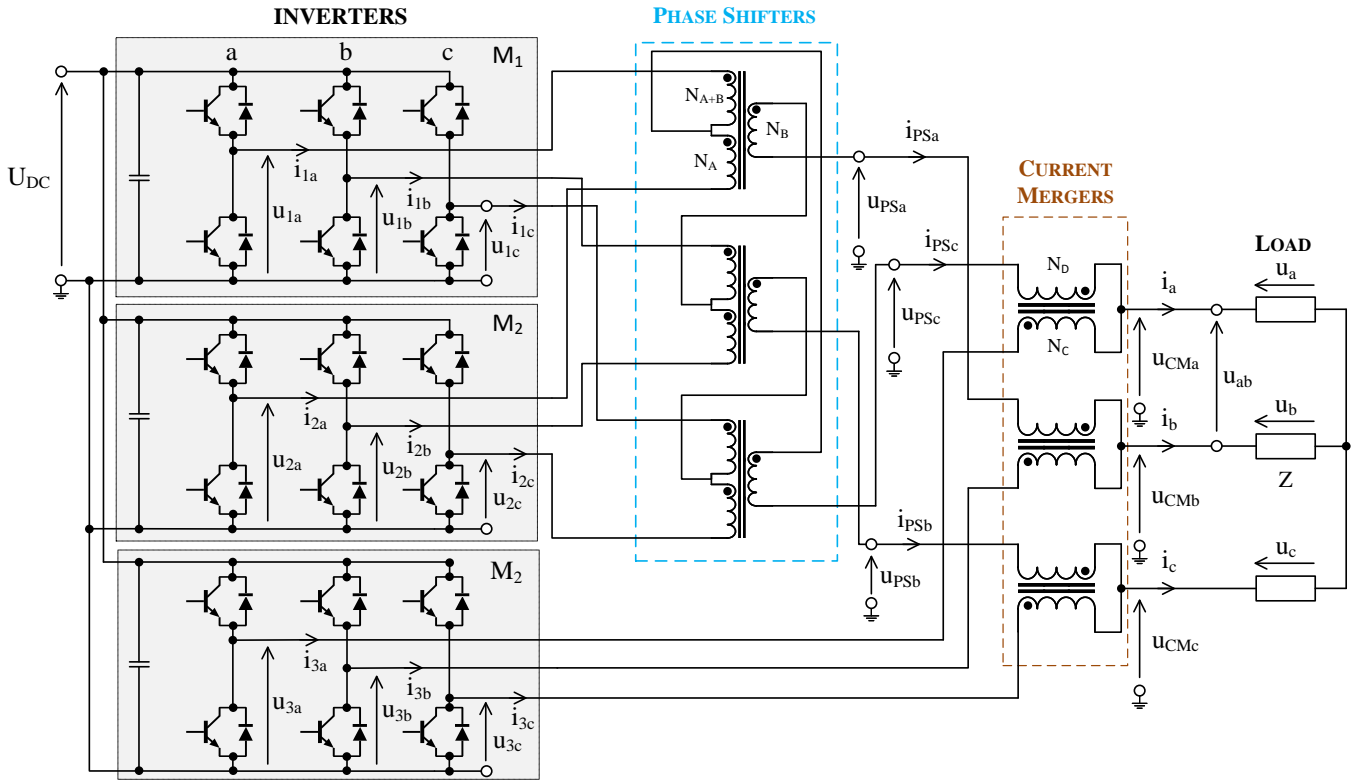*Bull. Pol. Acad. Sci. Tech. Sci.*, vol. 73, no. 4, p. e153227, 2025

Fig. 1. A multilevel voltage source inverter with phase shifters and current mergers based on 18-pulse topology
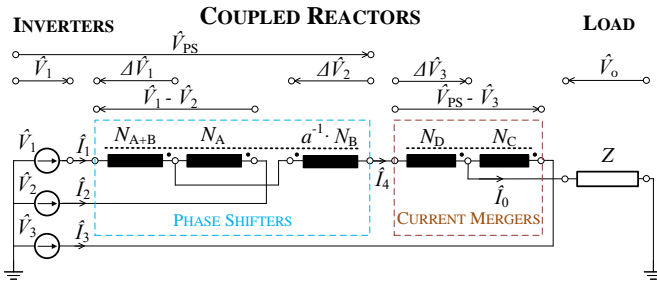

Fig. 2. Vectorial equivalent circuit of the multilevel voltage source inverter based on 18-pulse topology

phasor diagram shown in Fig. 3 (for $\phi = 20°$):

$$\frac{N_C}{N_D} = 2 \cdot \cos(\phi), \tag{9}$$

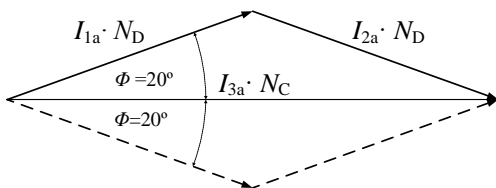where N_C and N_D refer to the primary and secondary windings of the current merger.

Fig. 3. The phasor diagram of the current merger

Taking into account the above relationships, the required turns ratios are found to be

$$\frac{N_A}{N_B} = 1.88,$$

$$\frac{N_C}{N_D} = 1.88. \tag{10}$$

The absolute numbers of turns depend on a variety of parameters, such as the inverter power, currents, output frequency, and the properties of the magnetic material. The details of the coupled reactors design are not in the scope of this article.

For the sake of implementation, it is convenient to express the vector equations in the matrix format. Based on equations (4) and (5), the voltages of the phase shifters can be expressed as

$$\begin{bmatrix} u_{PSa} \\ u_{PSb} \\ u_{PSc} \end{bmatrix} = \begin{bmatrix} u_{1b} & u_{1b} - u_{2b} & u_{1a} - u_{2a} \\ u_{1c} & u_{1c} - u_{2c} & u_{1b} - u_{2b} \\ u_{1a} & u_{1a} - u_{2a} & u_{1c} - u_{2c} \end{bmatrix} \cdot \begin{bmatrix} 1 \\ -k_1 \\ -k_2 \end{bmatrix} \tag{11}$$

while equation (7) (describing the voltage at the output of phase shifters and the inverter) can be converted to

$$\begin{bmatrix} u_{CMa} \\ u_{CMb} \\ u_{CMc} \end{bmatrix} = \begin{bmatrix} u_{3a} & u_{3a} - u_{PSa} \\ u_{3b} & u_{3b} - u_{PSb} \\ u_{3c} & u_{3c} - u_{PSc} \end{bmatrix} \cdot \begin{bmatrix} 1 \\ -k_3 \end{bmatrix}. \tag{12}$$

Bull. Pol. Acad. Sci. Tech. Sci., vol. 73, no. 4, p. e153227, 2025

3

Based on equations (4) and (3), the coefficients in the above equations can be calculated as

$$k_1 = \frac{N_A + N_B}{2 \cdot N_A + N_B} = 0.605,$$

$$k_2 = \frac{N_B}{2 \cdot N_A + N_B} = 0.2101, \tag{13}$$

$$k_3 = \frac{N_C}{N_C + N_D} = 0.6528.$$

The space-vector diagram – as shown in Fig. 4 – can be directly obtained using equation (12) and the Clarke transform

$$\begin{bmatrix} v_\alpha \\ v_\beta \end{bmatrix} = \begin{bmatrix} \frac{2}{3} & -\frac{1}{3} & -\frac{1}{3} \\ 0 & \frac{1}{\sqrt{3}} & -\frac{1}{\sqrt{3}} \end{bmatrix} \cdot \begin{bmatrix} u_{CMa} \\ u_{CMb} \\ u_{CMc} \end{bmatrix}. \tag{14}$$

The proposed topology, based on three conventional voltage source inverter modules, permits generation of AC voltages with variable amplitude and frequency. However, it is not an AC voltage source with a linear range of output voltage. In general, the output voltage hodograph can take the form of an eighteen-sided convex polygon (18-gon or *octadecagon*), and in some cases it can be a thirty-six-sided polygon (36-gon or *triacontahexagon*). The selection of inverter basic vectors essentially relies on the criterion of proximity between the reference vector and the available basic vectors. Moreover, appropriate use of redundant states should be made to minimize the switching frequency and optimize the reactor magnetic flux in phase shifters and current mergers.

4. COARSELY QUANTIZED PULSE AMPLITUDE MODULATION

The space-vector diagram of the 18-pulse topology consists of 512 inverter states in total, while the number of unique voltage vectors is equal to 343. Redundant inverter states have been analyzed and selected according to the minimum switching frequency and zero-average value of magnetic flux in the reactors. The magnetic flux has been estimated by simulation. Finally, the states have been grouped into collections corresponding to the modulation index defined by

$$m_a = \frac{V_{bv}}{U_{DC}}, \tag{15}$$

where V_{bv} stands for the magnitude of the basic inverter vector.

Table 1 shows the available modulation indices, the total number of corresponding states, the number of redundant states, and the number of switchings within the fundamental period. To each modulation index there corresponds its switch state table. The discrete regulation of the output voltage is possible from $m_a = 0.08$, which is 8% of the DC-link voltage, to $m_a = \frac{2}{3}$ which is 66.67% of the DC-link voltage.
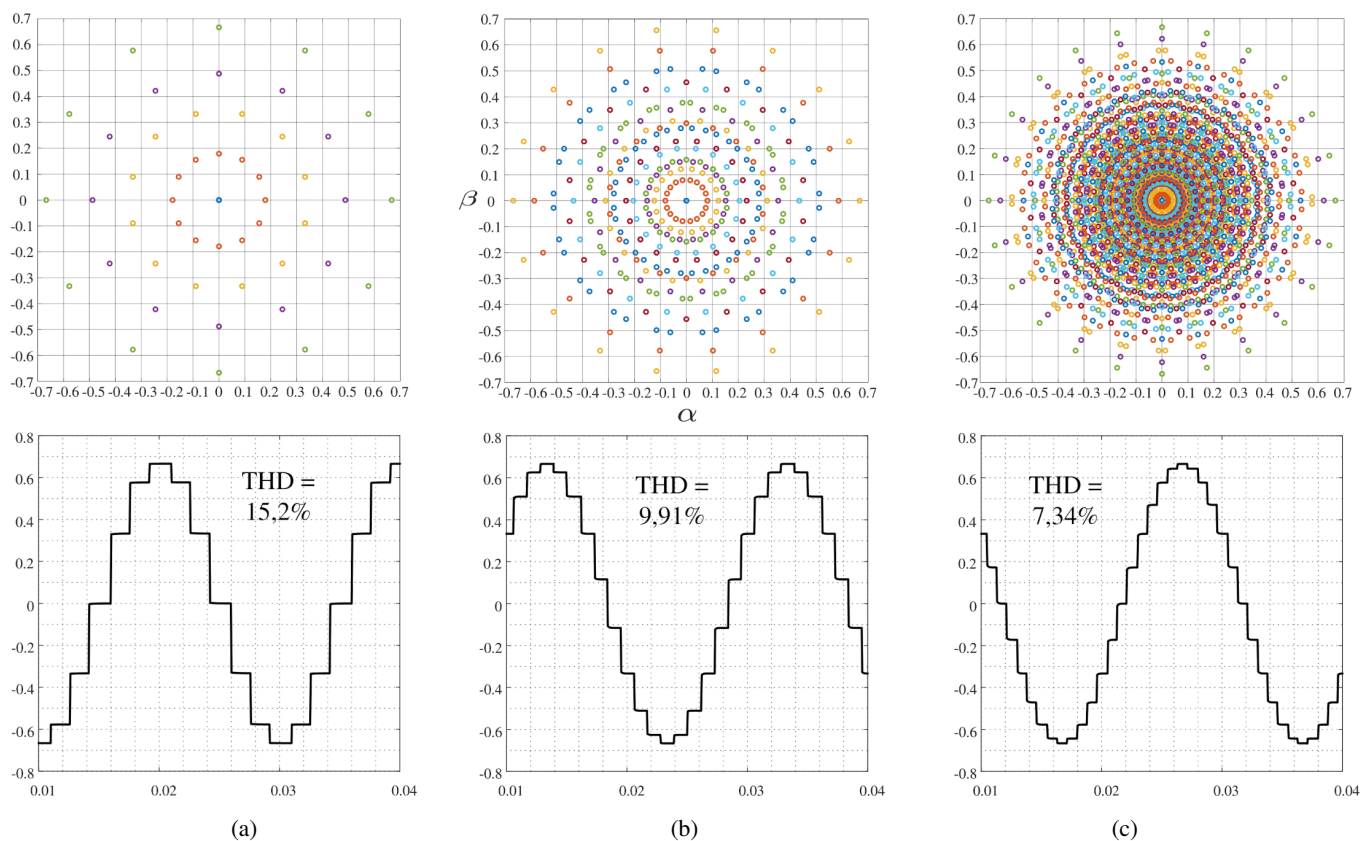

Fig. 4. Space-vector diagrams and the phase output voltages for multipulse systems: (a) 12-pulse, (b) 18-pulse, (c) 24-pulse

4

Bull. Pol. Acad. Sci. Tech. Sci., vol. 73, no. 4, p. e153227, 2025

Table 1

The properties of the modulation indices of the considered inverter

Modulation index m_a	Total number of states in the given collection	The number of subsets of redundant states	Total number of vectors in the subsets	The number of switchings within the fundamental period
0	8	8	1	|
0.0803	36	2	18	6
0.12296	18	1	18	5
0.1505	18	1	18	7
0.15826	36	2	18	5
0.2032	18	1	18	7
0.23	72	4	18	3
0.2802	36	1	36	9
0.2974	36	2	18	5
0.312	18	1	18	5
0.35464	36	2	18	4
0.37663	36	1	36	9
0.4349	36	2	18	4
0.456	36	2	18	3
0.51122	36	1	36	7
0.586	18	1	18	3
0.6667	18	1	18	1

The CQ-PAM switching sequence is performed according to the criterion of the minimum distance between the reference voltage vector v_{ref} and the available basic vectors. As a first step, an indicator ($p_{\min}$) of the appropriate collection of basic vectors is found based on the comparison between the magnitude of the reference vector V_{ref} and the available magnitudes of basic vectors:

$$p_{\min} = \underset{m_a}{\text{argmin}} \, |V_{\text{ref}} - m_a \cdot U_{\text{DC}}|. \quad (16)$$

Then, for the selected $p_{\min}$, the particular basic vector is selected based on the minimum-distance criterion:

$$(v_\alpha, v_\beta)_{\min} = \underset{(v_\alpha, v_\beta)}{\text{argmin}} \sqrt{(v_{\text{ref}_\alpha} - v_\alpha)^2 + (v_{\text{ref}_\beta} - v_\beta)^2}. \quad (17)$$

5. SIMULATION RESULTS

The proposed concept of MVSI-CR based on 18-pulse topology, shown in Fig. 1, has been verified using the PSIM11 simulation software and the Matlab environment. An important feature of the proposed solution is the ability to generate the multi-phase quasi sinusoidal output voltage. However, this is not a smooth regulation. The voltage amplitude can take one of 16 discrete values, which is illustrated in Fig. 5 (to achieve smooth amplitude regulation, the pulse width modulation techniques can be considered). Table 1 shows the number of switchings in the fundamental period of the generated waveform for each range of the output voltage.

The currents are shown in Fig. 6. As can be seen, all 6-pulse modules are equally loaded, which confirms the consistency of the proposed modularity concept. The synthesis principle of the load current in phase a is illustrated in Fig. 6; as can be seen, the currents are phase-shifted by $\phi = 20°$, as expected.
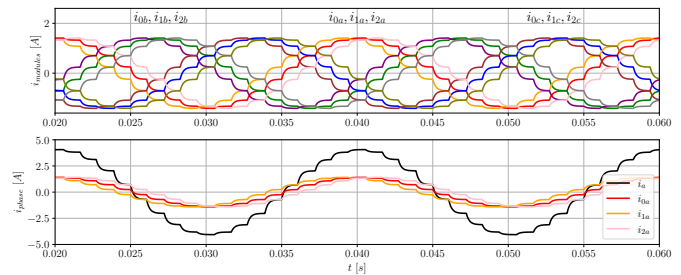
Fig. 6. Currents of the modular inverters and the phase a output current, and phase a modules currents

As mentioned in the previous section, redundant states exist for some modulation indices, which can be used for the control of
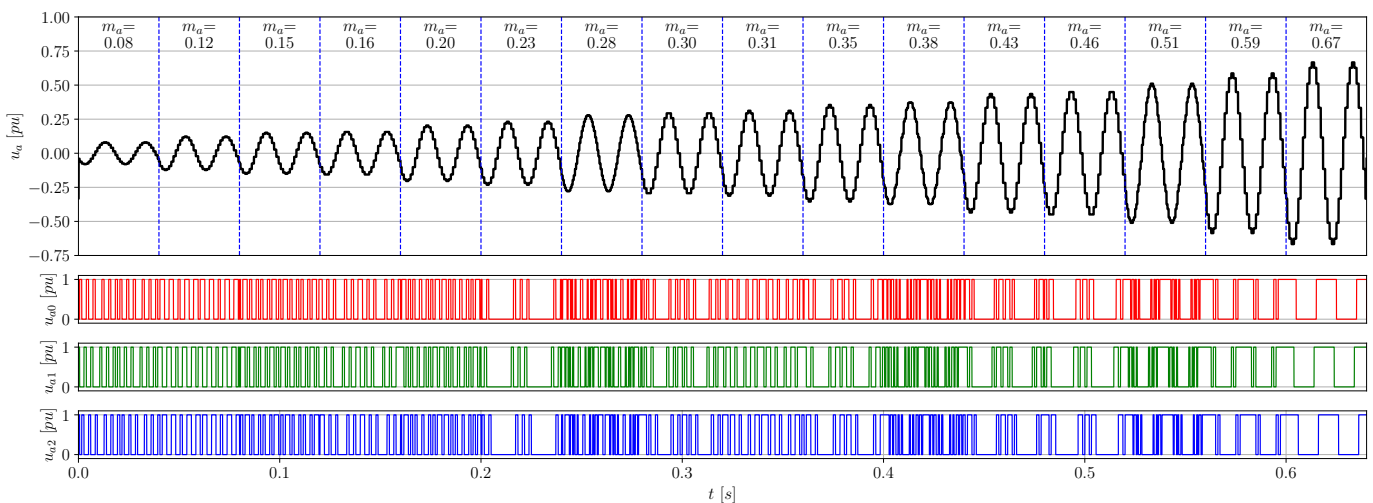
Fig. 5. Illustration of the output phase voltage levels

Bull. Pol. Acad. Sci. Tech. Sci., vol. 73, no. 4, p. e153227, 2025

5

magnetic flux in phase shifters and current mergers. All collections of basic vectors permit the average flux equal to 0 in every period of the output voltage. However, for some modulation indices the corresponding collections of basic vectors may include two or four subsets of redundant states (leading to the same output voltage, but different flux values as presented in Fig. 7. This property can be useful in the case of asymmetric loads.
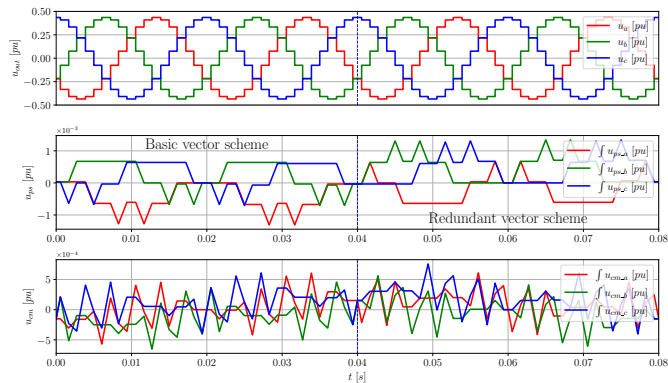

Fig. 7. Phase voltages for $m_a = 0.4349$, interpolated fluxes of CM and PS for basic vectors scheme, and scheme with redundant states

6. LABORATORY TEST RESULTS

Laboratory tests have been performed using the prototype of the MVSI-CR illustrated in Fig. 8. The most important circuit and control parameters have been presented in Table 2. The control board contains a two-core Texas Instruments digital signal processor TMS320C6672 and an Intel programmable logic device CYCLONE V. The presented coupled reactors have been designed for 50 Hz fundamental frequency. Obviously,
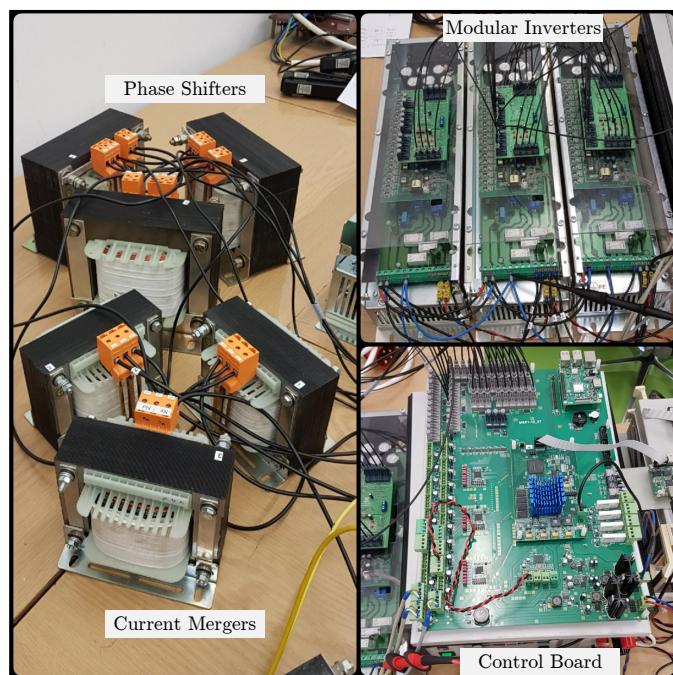
Fig. 8. A laboratory prototype of the 18-pulse inverter with coupled reactors

Table 2
Experiment circuit diagram and modulation parameters

Symbol	Value	Description
P_n	21.5 kW	Nominal total inverter power
U_{DC}	140 V	DC source voltage
R	15,6 Ω	Load resistor
L	3 mH	Load inductor
f_o	50 Hz, 200 Hz	Output frequencies
N_A	290	PS winding A turns
N_B	154	PS winding B turns
N_Σ	444	PS winding Σ turns
N_C	292	CM winding C turns
N_D	155	CM winding D turns

for greater fundamental frequencies these constructions will be much smaller. Measurements were taken by means of a Tektronix MDO4104B-3 Oscilloscope and a ZES Zimmer LMG670 Precision Power Analyzer. Three two-level inverters with nominal power of 7.5 kVA were used as modules M_0, M_1, and M_2 (cf. Fig. 1).

An important characteristic of the MVSI-CR system is the ability to immediately change the output voltage amplitude without undesirable transients, as presented in Fig. 9. As can be noticed, the rapid change from the minimum modulation index to the maximum value does not constitute a problem. In addition, the frequency of the generated voltage can be fully controlled. A rapid change in frequency is shown in Fig. 10. A fast change in the fundamental frequency can be useful in some high-frequency applications, such as induction heating.
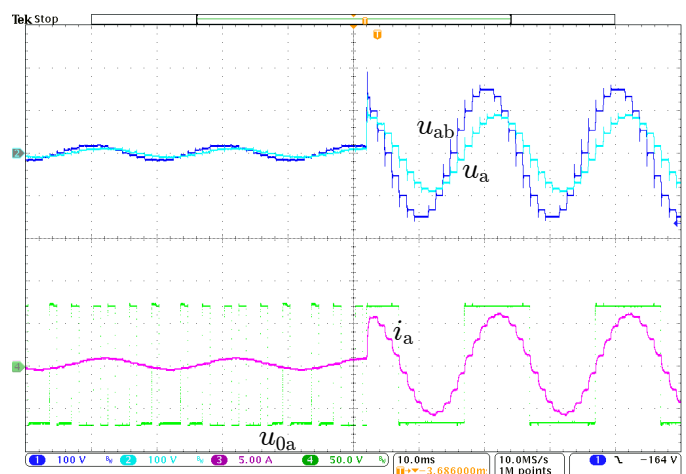

Fig. 9. Rapid change of the modulation index from the minimal to the maximal value

The proposed solution contains three identical inverters operating under similar conditions. The RMS values of inverter currents are the same for all modules. Example current waveforms of module M2 and the load current in phase a are shown in Fig. 11. Thus, the correct and balanced operation of all mod-

6

Bull. Pol. Acad. Sci. Tech. Sci., vol. 73, no. 4, p. e153227, 2025

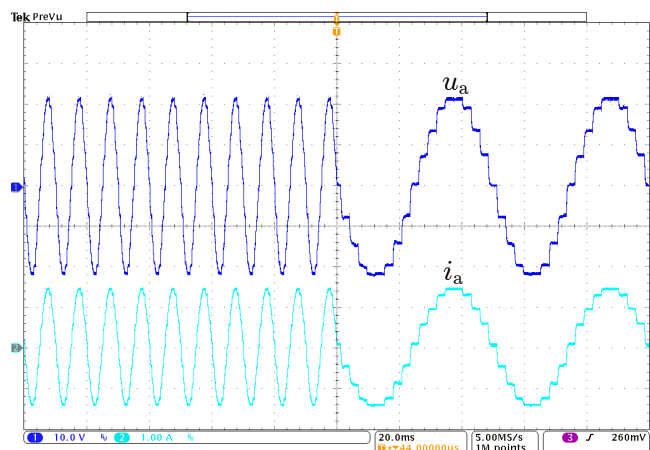Multilevel voltage source inverter with coupled reactors using CQPAM

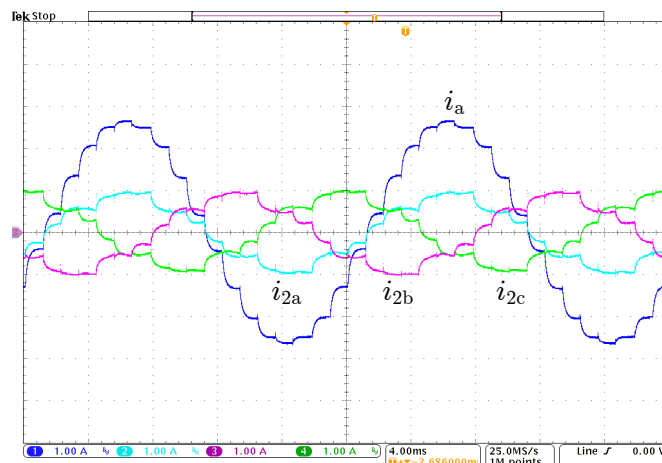**Fig. 10.** A rapid step-change of the reference frequency

**Fig. 11.** Phase a current and M_2 module currents of MVSI-CR for $m_a = 0.312$, $f_o = 50$ Hz

ules has been confirmed experimentally. Currents in the other modules look the same, except for the phase shift by ±20°.

Further tests were intended to verify correct operation of the proposed solution for two fundamental frequencies, 50 Hz and 200 Hz, and a full range of available modulation indices, from $m_a = 0.08$ to $m_a = 0.67$. For the sake of easy examination, the example waveforms are shown on one page.

All multi-pulse phase voltages, shown in Fig. 12, are formed according to the proposed approach of low-switching modulation. The overvoltage spikes observed in Fig. 13a and Fig. 13b

do not affect the load currents. Note that the magnitudes of the spikes are less than DC voltage and the results were obtained for very low reference voltage.

The harmonic spectra were also measured using a dedicated hardware analyzer. The results are shown in Fig. 12g for 50 Hz and Fig. 12h for 200 Hz, respectively. As predicted by the proposed formula (1), the 17th and 19th harmonics are the dominating distortion components. As expected, the THD value increases as the output voltage decreases. Notably, the 36-pulse voltage waveform exhibits a lower THD compared to the
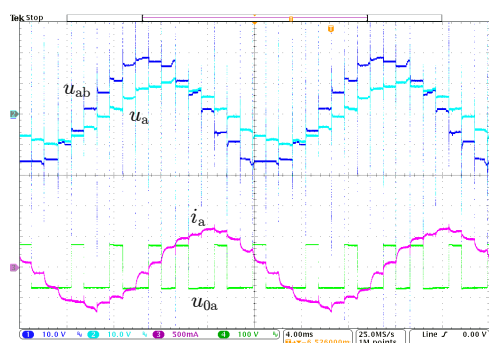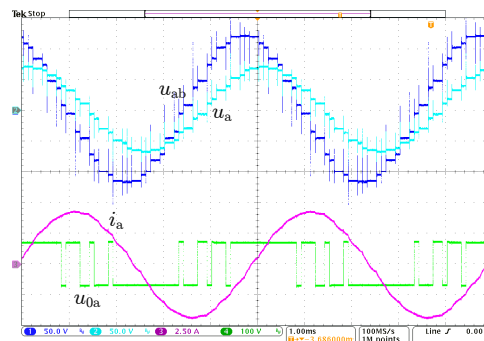

(a) $m_a = 0.08$, $f_o = 50$ Hz, 18-pulse phase voltage
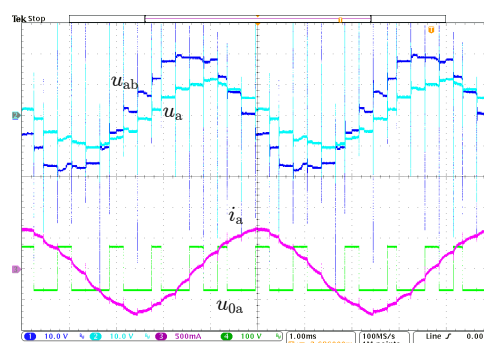
(b) $m_a = 0.08$, $f_o = 200$ Hz, 18-pulse phase voltage
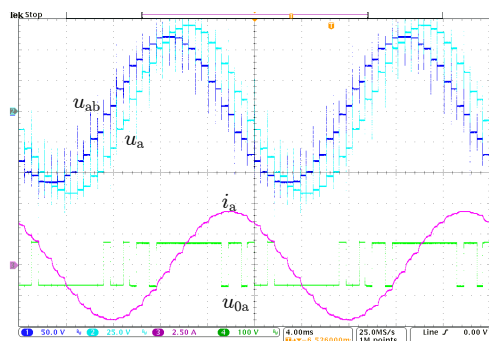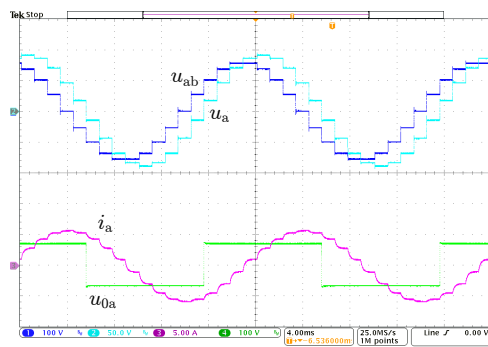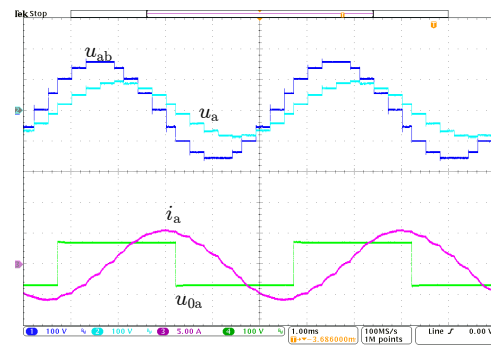

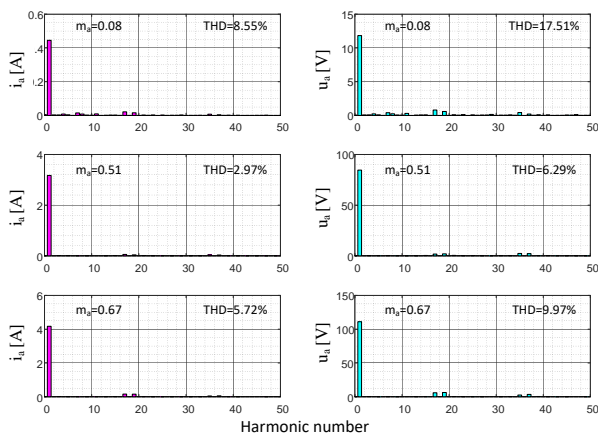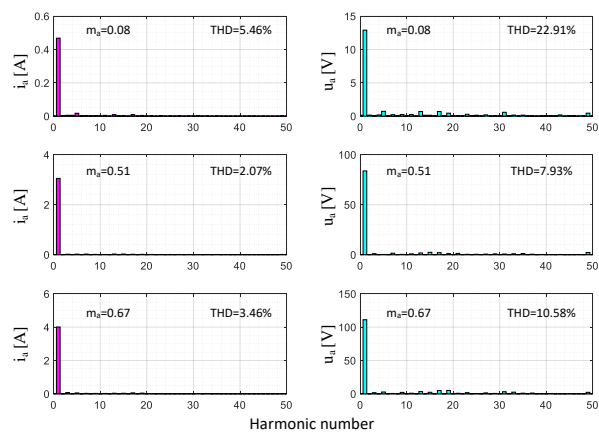**(c)** $m_a = 0.51$, $f_o = 50$ Hz, 36-pulse phase voltage

(d) $m_a = 0.51$, $f_o = 200$ Hz, 36-pulse phase voltage

Figure 12: (a)–(d)

Bull. Pol. Acad. Sci. Tech. Sci., vol. 73, no. 4, p. e153227, 2025

7

K.J. Szwarc, A. Cichowski, P. Szczepankowski, J. Nieznański, and R. Strzelecki

(e) $m_a = 0.67$, $f_o = 50$ Hz, 18-pulse phase voltage

(f) $m_a = 0.67$, $f_o = 200$ Hz, 18-pulse phase voltage

(g) Harmonics of phase current and voltage for $f_o = 50$ Hz

(h) Harmonics of phase current and voltage for $f_o = 200$ Hz

Fig. 12. Experimental results comparison for 50 Hz and 200 Hz

18-pulse output voltage waveform, even though there are more switch commutations per period at the 36-pulse case.

7. CONCLUSIONS

The discussed solution uses the multilevel voltage source inverter based on 18-pulse topology with two types of coupled reactor circuits – the phase shifters and the current mergers. An appropriate arrangement and connection of these circuits permit the multi-pulse synthesis and can be a justifiable alternative to the transformer-based solutions. The proposed inverter allows smooth frequency control and coarsely quantized amplitude regulation with low switching frequency, which means that it can be implemented using standard IGBT modules. This kind of topology can be an appropriate choice for a variety of high-frequency applications, notably those indicated in the introduction. The modularity of the MVSI-CR is an important advantage in its own right.

In the case of applications requiring precise amplitude control, a narrow-range DC-link regulation can be additionally employed. Alternatively, additional use of PWM or PDM can be considered. These aspects require further studies.

The practical application of the proposed concept also requires validation research, which includes the load asymmetry, the efficiency tests, the use of multi-level inverters as the MVSI-CR modules, or and the saturation phenomena.

REFERENCES

[1] F.R. Ismagilov, N. Uzhegov, V.E. Vavilov, V.I. Bekuzin, and V.V. Ayguzina, "Multidisciplinary design of ultra-high-speed electrical machines," *IEEE Trans. Energy Conv.*, vol. 33, no. 3, pp. 1203–1212, 2018, doi: 10.1109/TEC.2018.2803146.

[2] C. Zwyssig, M. Duerr, D. Hassler, and J. Kolar, "An ultra-high-speed, 500000 rpm, 1 kW electrical drive system," in *2007 Power Conversion Conference - Nagoya*, 2007, pp. 1577–1583, doi: 10.1109/PCCON.2007.373174.

[3] D. Gerada, A. Mebarki, N.L. Brown, C. Gerada, A. Cavagnino, and A. Boglietti, "High-speed electrical machines: Technologies, trends, and developments," *IEEE Trans. Ind. Electron.*, vol. 61, no. 6, pp. 2946–2959, 2014, doi: 10.1109/TIE.2013.2286777.

[4] J. Chivite-Zabalza, M.A. Rodríguez Vidal, P. Izurza-Moreno, G. Calvo, and D. Madariaga, "A large power, low-switching-frequency voltage source converter for facts applications with low effects on the transmission line," *IEEE Trans. Power Electron.*, vol. 27, no. 12, pp. 4868–4879, 2012, doi: 10.1109/TPEL.2012.2192753.

[5] K. Oguchi, G. Maeda, N. Hoshi, and T. Kubata, "Coupling rectifier systems with harmonic cancelling reactors," *IEEE Ind. Appl. Mag.*, vol. 7, no. 4, pp. 53–63, 2001, doi: 10.1109/2943.930991.

[6] B. Singh, S. Gairola, B.N. Singh, A. Chandra, and K. Al-Haddad, "Multipulse ac–dc converters for improving power quality: A review," *IEEE Trans. Power Electron.*, vol. 23, no. 1, pp. 260–281, 2008, doi: 10.1109/TPEL.2007.911880.

[7] P. Mysiak and R. Strzelecki, "A robust 18-pulse diode rectifier with coupled reactors," *Bull. Pol. Acad. Sci. Tech. Sci.*, vol. 59, no. 4, pp. 541–550, 2011, doi: 10.2478/v10175-011-0066-2.

[8] R. Strzelecki, T. Sak, and N. Strzelecka, "Method and system to converting of electrical energy with the use of multilevel inverters connected in parallel," Polish Patent PL 228 547, April 30, 2018.

[9] R. Strzelecki, T. Sak, P. D. Zolov, A. Moradewicz, and M. Grabarek, "Multi-pulse vsc arrangements with coupled reactors," in *2016 IEEE 2nd Annual Southern Power Electronics Conference (SPEC)*, 2016, pp. 1–6, doi: 10.1109/SPEC.2016.7846037.

[10] A. Pietkiewicz and H.-P. Biner, "Novel low harmonic three-phase 12-pulse inverter," in *International Symposium on Power Electronics Power Electronics, Electrical Drives, Automation and Motion*, 2012, pp. 837–842, doi: 10.1109/SPEEDAM.2012.6264488.

[11] B. Geethalakshmi, P. Dananjayan, and K. DelhiBabu, "A combined multipulse-multilevel voltage source inverter configuration for statcom applications," in *2008 Joint International Conference on Power System Technology and IEEE Power India Conference*, 2008, pp. 1–5, doi: 10.1109/ICPST.2008.4745357.

[12] J. Biela, D. Hassler, J. Schönberger, and J.W. Kolar, "Closed-loop sinusoidal input-current shaping of 12-pulse autotransformer rectifier unit with impressed output voltage," *IEEE Trans. Power Electron.*, vol. 26, no. 1, pp. 249–259, 2011, doi: 10.1109/TPEL.2010.2052633.

[13] K. Mino, G. Gong, and J. Kolar, "Novel hybrid 12-pulse boost-type rectifier with controlled output voltage," *IEEE Trans. Aerospace Electron. Syst.*, vol. 41, no. 3, pp. 1008–1018, 2005, doi: 10.1109/TAES.2005.1541445.

[14] I. Araujo-Vargas, A.J. Forsyth, and F.J. Chivite-Zabalza, "Capacitor voltage balancing techniques for a multi-pulse pulse rectifier with active injection," in *2009 Twenty-Fourth Annual IEEE Applied Power Electronics Conference and Exposition*, 2009, pp. 383–389, doi: 10.1109/APEC.2009.4802686.

[15] G.-E. April and G. Olivier, "A novel type of 12-pulse converter," *IEEE Trans. Ind. Appl.*, vol. IA-21, no. 1, pp. 180–191, 1985, doi: 10.1109/TIA.1985.349679.

[16] Y. Voitovych, V. Makarov, and I. Pichkalov, "18-pulse rectifier with electronic phase shifting with autotransformer in inverter and rectifier mode," in *2018 IEEE 6th Workshop on Advances in Information, Electronic and Electrical Engineering (AIEEE)*, 2018, pp. 1–5, doi: 10.1109/AIEEE.2018.8592446.

[17] B. Wu, Y. Li, and S. Wei, "Multipulse diode rectifiers for high-power multilevel inverter fed drives," in *9th IEEE International Power Electronics Congress, 2004. CIEP 2004*, 2004, pp. 9–14, doi: 10.1109/CIEP.2004.1437533.

[18] A.N. Arvindan, R. Ashwin, and M.K. Murthi, "Multipulse diode rectifiers: Power quality perspective based on experimental data," in *2018 8th IEEE India International Conference on Power Electronics (IICPE)*, 2018, pp. 1–6, doi: 10.1109/IICPE.2018.8709575.

[19] F.C. Baiceanu, F. Munteanu, and C. Nemes, "Influence of multi-pulse rectifier on power quality in an industrial environment," in *2019 8th International Conference on Modern Power Systems (MPS)*, 2019, pp. 1–6, doi: 10.1109/MPS.2019.8759775.

[20] A. Gbadega Peter and A. Saha, "The impacts of harmonics reduction on thd analysis in hvdc transmission system using three-phase multi-pulse and higher level converters," in *2019 Southern African Universities Power Engineering Conference/Robotics and Mechatronics/Pattern Recognition Association of South Africa (SAUPEC/RobMech/PRASA)*, 2019, pp. 444–449, doi: 10.1109/RoboMech.2019.8704743.

[21] T. Yang, S. Bozhko, and G. Asher, "Functional modeling of symmetrical multipulse autotransformer rectifier units for aerospace applications," *IEEE Trans. Power Electron.*, vol. 30, no. 9, pp. 4704–4713, 2015, doi: 10.1109/TPEL.2014.2364682.

[22] Y. Zhang, Z. Chen, B. Li, and Y. He, "Application of low harmonic 18-pulse rectifier power supply for radar power system," *IEEE Trans. Ind. Electron.*, vol. 66, no. 2, pp. 1080–1088, 2019, doi: 10.1109/TIE.2018.2831188.

[23] F. Meng, Q. Du, L. Wang, L. Gao, and Z. Man, "A series-connected 24-pulse rectifier using passive voltage harmonic injection method at dc-link," *IEEE Trans. Power Electron.*, vol. 34, no. 9, pp. 8503–8512, 2019, doi: 10.1109/TPEL.2018.2889507.

[24] D. Raja, N. Muraly, V. Vijayavelan, and N. Selvaganesan, "A 24-pulse ac-dc converter for improving power quality using fork connected transformer," in *2009 International Conference on Control, Automation, Communication and Energy Conservation*, 2009, pp. 1–8.

[25] B. Singh and P. Kant, "A 54-pulse ac-dc converter fed 15-level inverter based vector controlled induction motor drive," in *2017 IEEE Industry Applications Society Annual Meeting*, 2017, pp. 1–7, doi: 10.1109/IAS.2017.8101742.

[26] B. Geethalakshmi, T. Hajmunnisa, and P. Dananjayan, "Dynamic characteristic analysis of sssc based on 48-pulse inverter," in *2007 International Power Engineering Conference (IPEC 2007)*, 2007, pp. 550–554.

[27] M. Abolhassani, "Modular multipulse rectifier transformers in symmetrical cascaded h-bridge medium voltage drives," *IEEE Trans. Power Electron.*, vol. 27, no. 2, pp. 698–705, 2012, doi: 10.1109/TPEL.2011.2161593.

[28] I. Araujo-Vargas, A.J. Forsyth, and F.J. Chivite-Zabalza, "Capacitor voltage-balancing techniques for a multipulse rectifier with active injection," *IEEE Trans. Ind. Appl.*, vol. 47, no. 1, pp. 185–198, Jan 2011, doi: 10.1109/TIA.2010.2091475.

[29] M. Calar, E. Durna, and K. Kayisli, "3-phase multi-pulse rectifiers with different phase shifting transformers and comparison of total harmonic distortion," in *2022 9th International Conference on Electrical and Electronics Engineering (ICEEE)*, 2022, pp. 60–64, doi: 10.1109/ICEEE55327.2022.9772606.

[30] R.C. Fernandes, P. da Silva Oliveira, and F.J.M. de Seixas, "A family of autoconnected transformers for 12- and 18-pulse converters—generalization for delta and wye topologies," *IEEE Trans. Power Electron.*, vol. 26, no. 7, pp. 2065–2078, 2011, doi: 10.1109/TPEL.2010.2102773.

[31] D. Yuan, S. Wang, H. Li, S. Wang, and S. Wang, "Simulation analysis and development of industrial design software of phase-shifting reactor used in the 6-phase rectifier system," in *2017 20th International Conference on Electrical Machines and Systems (ICEMS)*, 2017, pp. 1–5, doi: 10.1109/ICEMS.2017.8056474.

[32] P. Szczepankowski, J. Luszcz, A. Usoltsev, N. Strzelecka, and E. Romero-Cadaval, "The conceptual research over low-switching modulation strategy for matrix converters with the coupled reactors," *Energies*, vol. 14, no. 3, p. 675, 2021, doi: 10.3390/en14030675.

[33] K.J. Szwarc, P. Szczepankowski, J. Nieznański, C. Swinarski, A. Usoltsev, and R. Strzelecki, "Hybrid modulation for modular voltage source inverters with coupled reactors," *Energies*, vol. 13, no. 17, p. 4450, 2020, doi: 10.3390/en13174450.

Bull. Pol. Acad. Sci. Tech. Sci., vol. 73, no. 4, p. e153227, 2025

9